VEGFR-3 controls tip to stalk conversion at vessel fusion sites by reinforcing Notch signalling

Published in final edited form as:
Nat Cell Biol. ; 13(10): 1202–1213. doi:10.1038/ncb2331.

VEGFR-3 controls tip to stalk conversion at vessel fusion sites by reinforcing Notch signalling

Tuomas Tammela[1,9], **Georgia Zarkada**[1,9], **Harri Nurmi**[1], **Lars Jakobsson**[2,10], **Krista Heinolainen**[1], **Denis Tvorogov**[1], **Wei Zheng**[1], **Claudio A. Franco**[2], **Aino Murtomäki**[1], **Evelyn Aranda**[3], **Naoyuki Miura**[4], **Seppo Ylä-Herttuala**[5], **Marcus Fruttiger**[6], **Taija Mäkinen**[1,10], **Anne Eichmann**[7], **Jeffrey W. Pollard**[3], **Holger Gerhardt**[2,8], and **Kari Alitalo**[1,11]

[1]Molecular/Cancer Biology Laboratory, Institute for Molecular Medicine Finland, Research Programs Unit and Department of Pathology, Haartman Institute, Biomedicum Helsinki, PO Box 63 (Haartmaninkatu 8), 00014 University of Helsinki, Finland [2]Vascular Biology Laboratory, London Research Institute—Cancer Research UK, 44 Lincoln's Inn Fields, London WC2A 3PX, UK [3]Department of Developmental and Molecular Biology, Albert Einstein College of Medicine, New York, New York 10461, USA [4]Department of Biochemistry, Hamamatsu University School of Medicine, 431-3192 Hamamatsu, Japan [5]A. I. Virtanen Institute and Department of Medicine, University of Kuopio, PO Box 1627, 70211 Kuopio, Finland [6]Institute of Ophthalmology, University College London, London EC1V 9EL, UK [7]Institut National de la Santé et de la Recherche Médicale U833, Collège de France, 11 Place Marcelin Berthelot, 75005 Paris, France [8]Vascular Patterning Laboratory, Vesalius Research Center, VIB, Campus Gasthuisberg, B-3000 Leuven, Belgium

Abstract

Angiogenesis, the growth of new blood vessels, involves specification of endothelial cells to tip cells and stalk cells, which is controlled by Notch signalling, whereas vascular endothelial growth factor receptor (VEGFR)-2 and VEGFR-3 have been implicated in angiogenic sprouting. Surprisingly, we found that endothelial deletion of *Vegfr3*, but not VEGFR-3-blocking antibodies, postnatally led to excessive angiogenic sprouting and branching, and decreased the level of Notch signalling, indicating that VEGFR-3 possesses passive and active signalling modalities.

[11]Correspondence should be addressed to K.A. (Kari.Alitalo@Helsinki.Fi).
[9]These authors contributed equally to this work.
[10]Present addresses: Vascular Biology, Department of Medical Biochemistry and Biophysics, Karolinska Institutet, Scheeles Väg 2, SE171 77 Stockholm, Sweden (L.K.); Lymphatic Development Laboratory, Cancer Research UK London Research Institute, 44 Lincoln's Inn Fields, London WC2A 3PX, UK (T.M.).

Note: Supplementary Information is available on the Nature Cell Biology website

AUTHOR CONTRIBUTIONS

T.T. and G.Z. designed, directed and carried out experiments and data analysis, as well as interpreted results, and wrote the paper; H.N. designed and carried out cell culture and biochemistry experiments, and analysed data; L.J. carried out three-dimensional embryoid body sprouting experiments and analysed data; K.H. carried out cell culture, morphometry of retinal vessels and qRT-PCR, and analysed data; D.T. carried out biochemistry experiments and analysed data; W.Z. produced and validated Notch ligand and inhibitor proteins; C.A.F. carried out three-dimensional embryoid body sprouting experiments and analysed data; A.M. carried out retina experiments and analysed data; E.A. provided *op/op* retinas and carried out genotyping; N.M. generated FoxC2 antibodies; S.Y-H. generated adenoviral vectors; M.F. generated $Pdgfb CreER^{T2}$ mice; T.M. generated $Vegfr3^{flox/flox}$ mice; A.E. analysed retinas of $Vegfr3^{+/LacZ}$ mice; J.W.P. provided *op/op* retinas; H.G. directed experiments, interpreted results and helped write the paper; K.A. designed and directed experiments, interpreted results and wrote the paper.

COMPETING FINANCIAL INTERESTS

K.A. is the chairman of the Scientific Advisory Board of Circadian.

Furthermore, macrophages expressing the VEGFR-3 and VEGFR-2 ligand VEGF-C localized to vessel branch points, and *Vegfc* heterozygous mice exhibited inefficient angiogenesis characterized by decreased vascular branching. FoxC2 is a known regulator of Notch ligand and target gene expression, and $Foxc2^{+/-}$; $Vegfr3^{+/-}$ compound heterozygosity recapitulated homozygous loss of *Vegfr3*. These results indicate that macrophage-derived VEGF-C activates VEGFR-3 in tip cells to reinforce Notch signalling, which contributes to the phenotypic conversion of endothelial cells at fusion points of vessel sprouts.

During late embryogenesis and in the adult, blood vessels form primarily by angiogenesis, that is by sprouting from pre-existing vessels. Vascular endothelial growth factor (VEGF) potently promotes angiogenesis, and is indispensable for vascular development[1,2], and VEGFR-2 tyrosine kinase is the primary receptor transmitting VEGF signals in endothelial cells[3,4]. VEGFR-3 is activated by the VEGF homologues VEGF-C and VEGF-D, which, when fully proteolytically processed, also stimulate VEGFR-2 (ref. 5) and induce the formation and activation of VEGFR-2–VEGFR-3 heterodimers[6,7]. Inactivation of the *Vegfr3* gene (also known as *Flt4*) leads to marked defects in arterial–venous remodelling of the primary vascular plexus, resulting in lethality by embryonic day (E) 10.5 (ref. 8) or to defective segmental artery morphogenesis[9] in mice or zebrafish, respectively.

As the lymphatic vessels begin to develop at around E10.5, the level of *Vegfr3* expression gradually decreases in the blood vessels, and from E16.5 onwards it is found nearly exclusively in the lymphatic vascular endothelium[10,11]. However, VEGFR-3 is induced in angiogenic endothelial cells for example in tumours, wounds and in maturing ovarian follicles[12–14]. Homozygous gene-targeting of *Vegfc* leads to embryonic lethality at E16.5 due to a complete failure in lymphatic vessel formation, whereas *Vegfc* heterozygous mice survive with lymphatic vessel hypoplasia and lymphedema, but do not exhibit blood vascular defects as adults[15]. Conversely, *Vegfd* gene-targeted mice are viable and normal[16]. Interestingly, compound deletion of both *Vegfc* and *Vegfd* phenocopies the homozygous loss of *Vegfc*, but these mice survive past the time point of critical requirement for *Vegfr3* (ref. [17]), implicating other as yet unknown ligands or ligand-independent signalling for VEGFR-3.

Angiogenic sprouting involves specification of subpopulations of endothelial cells into tip cells that respond to VEGF guidance cues, and stalk cells that follow the tip cells and proliferate to form the vascular network[18]. Recent evidence indicates that VEGF induces the membrane-bound Notch ligand delta-like 4 (Dll4) in the tip cells, which leads to the induction of the stalk-cell phenotype in adjacent endothelial cells through activation of Notch-1 (refs 10,19–21). The angiogenic sprouts fuse at intervals[18], followed by the formation of a vessel lumen to form a functional microcirculatory loop[22,23]. The fusion of migrating tip cells is chaperoned by Tie2- and neuropilin-1-positive macrophages[24], which express a variety of growth factors and proteolytic enzymes[24–26]. However, the molecular players regulating sprout fusion and vessel anastomosis have remained unknown.

We recently demonstrated that VEGFR-3 is expressed at a high level in endothelial tip cells, and that blocking VEGFR-3 with antibodies results in decreased angiogenesis during postnatal development and in tumours[14]. Stimulation of VEGFR-3 augments VEGF-induced angiogenesis and sustains blood vessel growth even in the presence of VEGFR-2 inhibitors, whereas antibodies against VEGFR-3 and VEGFR-2 in combination produce additive inhibition of angiogenesis and tumour growth[14]. Consistent with the concept of high levels of VEGFR-3 activity in the tip cells, genetic or pharmacological disruption of the Notch signalling pathway *in vivo* leads to widespread endothelial *Vegfr3* expression and excessive sprouting[14,27,28].

Here, we show that genetic inactivation of *Vegfr3* in endothelial cells surprisingly resulted in increased numbers of tip cells and vessel hyperplasia, which closely resembled loss of Notch signalling, whereas haploinsufficiency of *Vegfc* led to disruption of tip cell fusion points and inefficient angiogenesis. Our results implicate a bimodal role for VEGFR-3 in regulating angiogenesis, and indicate that the VEGF-C–VEGFR-3 signalling pathway controls the branching morphogenesis of blood vessels.

RESULTS

Endothelial deletion of *Vegfr3* results in excessive angiogenesis

To study the consequences of homozygous endothelial-specific loss of *Vegfr3* during angiogenesis, we mated $Vegfr3^{flox/flox}$ mice with $PdgfbiCreER^{T2}$ mice that express tamoxifen-activated Cre recombinase in endothelial cells[29]. Complete deletion of *Vegfr3* in the retinal endothelium was achieved by 24 h following administration of 4-hydroxytamoxifen (4-OHT; Supplementary Fig. S1a–d). Some residual *Vegfr3* expression was detected by quantitative real-time (qRT) PCR (Supplementary Fig. S1e), presumably originating from retinal oligodendrocytes[30] or from monocytic cells[31].

Surprisingly, when Cre was induced in $PdgfbiCreER^{T2}$; $Vegfr3^{flox/flox}$ ($Vegfr3^{i\Delta EC}$) mice for 48 h from postnatal day (P) 3 to P5, marked excessive branching, filopodia projection and hyperplasia of the nascent vascular plexus were observed (Fig. 1a–e). There was a significant increase in the proliferation of retinal endothelial cells (Fig. 1f and Supplementary Fig. S2). Increased branching and vascular hyperplasia were also observed in hindbrains of $Vegfr3^{i\Delta EC}$ embryos at E11.5 (Fig. 1g–k and Supplementary Fig. S3).

We sought to validate these findings in other models outside the developing central nervous system. Excessive angiogenesis and sprouting were also detected in syngeneic subcutaneously implanted Lewis lung carcinomas (LLC) and B16-F10 melanomas in the $Vegfr3^{i\Delta EC}$ mice (Fig. 1l,m and data not shown). Furthermore, when ears of adult $Vegfr3^{i\Delta EC}$ mice were transduced with AdVEGF, we observed a more robust angiogenic response, characterized by increased vascular tortuosity, enlargement and surface area (Fig. 1n and Supplementary Fig. S4).

VEGFR-3 tyrosine kinase activity is crucial for lymphatic vessel growth[32], but its role in angiogenesis is not known. To determine whether VEGFR-3 is tyrosine phosphorylated in blood vascular endothelial cells *in vivo*, we injected recombinant VEGF, VEGF-C or BSA control protein into the outflow tract of wild-type embryos at E10.5, a stage when lymphatic vessels have not yet developed (Fig. 2a–c). VEGF did not promote tyrosine phosphorylation of VEGFR-3, unlike VEGF-C, but a faint phosphorylation signal was detected in both VEGF- and BSA-stimulated embryos, indicating a baseline level of VEGFR-3 phosphorylation (Fig. 2b). As expected, VEGF and VEGF-C both stimulated VEGFR-2 phosphorylation (Fig. 2c).

We have previously shown that VEGFR-3-blocking antibodies suppress angiogenesis[14], whereas our results surprisingly showed that genetic targeting of *Vegfr3* produced excessive angiogenic sprouting, indicating the possibility of ligand-independent sprouting. We found that VEGFR-3 was phosphorylated in the absence of its ligands by stimulation with collagen I in cultured human dermal blood vascular endothelial cells (hBECs) even in the presence of blocking monoclonal antibodies or a VEGFR tyrosine kinase inhibitor, whereas the Src inhibitor PP2 blocked collagen-I-induced phosphorylation of VEGFR-3 (Fig. 2d), indicating that VEGFR-3 can be phosphorylated independently of its ligands[33].

We addressed the role of VEGFR-3 kinase activity in angiogenesis *in vivo* by studying the retinas of *Chy* mice, which harbour a heterozygous kinase-inactivating point mutation in the tyrosine kinase domain (*Vegfr3*$^{KD/+}$), leading to a decreased level of VEGFR-3 signalling and severe lymphatic vessel hypoplasia[32]. The retinas of mice harbouring one kinase-dead (KD) and one deleted *Vegfr3* allele (*Vegfr3*$^{i\Delta EC/KD}$) showed an increase in the vascular area, branching and filopodia projection that was comparable to homozygous loss of *Vegfr3* (*Vegfr3*$^{i\Delta EC/i\Delta EC}$; Fig. 2e–i), indicating that VEGFR-3 hypophosphorylation can trigger the phenotype. In contrast, *Vegfr3*$^{KD/+}$ and *Vegfr3*$^{i\Delta EC/+}$ single heterozygotes were indistinguishable from wild-type retinas (Fig. 2e–i).

The administration of VEGFR-3-blocking antibodies to *Vegfr3*$^{i\Delta EC}$ mice did not affect the hypervascular phenotype (Fig. 3a,b). In contrast, VEGFR-2-blocking antibodies rescued the increase in vascular area in the *Vegfr3*$^{i\Delta EC}$ mice (Fig. 3a,b). However, the nascent vessels appeared abnormally thick in the *Vegfr3*$^{i\Delta EC}$ retinas following administration of VEGFR-2-blocking antibodies (arrowheads in Fig. 3a), indicating that the phenotypic rescue was not complete. Furthermore, the expression level of VEGFR-1, a negative regulator of VEGF, was decreased in the *Vegfr3*$^{i\Delta EC}$ retinas (Fig. 3c), indicating an increased level of VEGF–VEGFR-2 signalling. Consistently, we detected a minor increase in the level of VEGFR-2 phosphorylation following stimulation of cultured human umbilical vein endothelial cells (HUVECs) with VEGF when VEGFR-3 expression was silenced using siRNA oligonucleotides (Fig. 3d). Antibodies blocking human VEGFR-3 had no effect on VEGFR-2 phosphorylation in response to VEGF in HUVECs (Supplementary Fig. S5a).

Loss of *Vegfr3* in endothelial cells leads to a decreased level of Notch target gene expression

The phenotype resulting from endothelial *Vegfr3* deletion closely resembled the hyperplastic vascular pattern resulting from inhibition of Dll4/Notch signalling between tip and stalk cells. Indeed, we detected a marked decrease in the level of Notch target gene transcripts and the Notch ligand *Dll4* in the *Vegfr3*$^{i\Delta EC}$ retinas (Fig. 4a), indicating a decreased level of Notch signalling in the endothelium, resulting in tip cell dominance over stalk cells. In contrast, no changes in Notch targets could be observed in pups treated with VEGFR-3-blocking antibodies (Supplementary Fig. S5b), indicating that the perturbations to VEGFR-3 by blocking antibodies and genetic targeting are qualitatively different.

To investigate the responsiveness of the *Vegfr3*-deficient endothelium to exogenous Notch activation, we administered Jagged1, a small peptide Notch agonist, to *Vegfr3*$^{i\Delta EC}$ pups, and observed a rescue of the hypervascular phenotype (Fig. 4b,c). Notably, the vasculature was normalized also in terms of morphology, unlike after anti-VEGFR-2 antibody administration (Fig. 4c), indicating that decreased Notch signalling underlies the phenotype in *Vegfr3*$^{i\Delta EC}$ retinas.

According to our results, VEGFR-3 contributes to the activation of Notch that is known to promote a phenotypic switch from a tip cell to a stalk cell. We chose to test this hypothesis in mosaic embryoid bodies consisting of both *Vegfr3*$^{+/LacZ}$ heterozygous and wild-type embryonic stem cells[34]. *Vegfr3*$^{+/LacZ}$ endothelial cells preferentially localized to the tips of VEGF-induced vascular sprouts (Fig. 4d,g), whereas inhibiting Notch cleavage with the γ-secretase inhibitor DAPT abrogated the competitive advantage of the *Vegfr3*$^{+/LacZ}$ endothelial cells (Fig. 4h). *Vegfr3*$^{+/LacZ}$ endothelial cells preferentially localized to the tips of vascular sprouts also in mosaic retinas at P5 (Fig. 4i), indicating increased tip cell competence for the *Vegfr3* haploinsufficient cells, which further implicates a decreased level of Notch signalling in endothelial cells with targeted *Vegfr3* loss-of-function.

VEGF-C–VEGFR-3 signalling controls fusion of vascular sprouts

We next sought to determine which of the two VEGFR-3 ligands, VEGF-C or VEGF-D, is responsible for activating VEGFR-3 in the angiogenic endothelium *in vivo*. Strikingly, *Vegfc* heterozygous mice demonstrated retardation of retinal vascularization and decreased vessel branching density (Fig. 5a–d). In contrast, the *Vegfc* heterozygotes exhibited increased vessel sprouting and filopodia projection (Fig. 5e,f), and a decrease in the level of Notch target gene expression (Fig. 5g). These results implied a failure in stabilization of sprout fusion sites, and indicated that the excess sprouts represent failed tip cell fusions. Indeed, tracking endothelial cell migration paths by collagen IV immunostaining showed that endothelial cells in *Vegfc*-haploinsufficient mice had frequently retracted from putative sprout fusion sites (Fig. 5h,i). Importantly, *Vegf* (also known as *Vegfa*) levels in the *Vegfc* heterozygous retinas were normal, whereas *Vegfc* transcript levels were decreased by more than 50% (Supplementary Fig. S5c). No changes in angiogenesis were observed in homozygous or heterozygous *Vegfd* gene-targeted retinas (Supplementary Fig. S6), indicating that VEGF-C is the key ligand responsible for VEGFR-3 activation during retinal angiogenesis.

Macrophages expressing Tie2 have been implicated as critical cellular chaperones for the formation of vascular anastomoses[24,25], and our results indicated a role for VEGF-C in this process. We detected VEGF-C expression in 50.9% (3.1% ± s.e.m.) of F4/80-positive macrophages in wild-type retinas. High-resolution imaging showed that all F4/80- and Tie2-positive cells were also VEGF-C positive (Fig. 5j). Curiously, the VEGF-C-positive macrophages were positioned at the vascular front and primarily resided at vascular branching points immediately behind the tip cell front, whereas macrophages at sites of tip cell engagement expressed lower levels of VEGF-C (Fig. 5j and Supplementary Fig. S7).

Interestingly, complete loss of macrophages in *op/op* mice[35] largely phenocopied heterozygous loss of *Vegfc*, as evidenced by decreased radial migration, area and branching of the vascular plexus, as well as by increased sprouting of the vessels (Fig. 5k–o). Furthermore, the Notch target genes *Hey1* and *Hey2* were significantly downregulated in the *op/op* retinas (Fig. 5p).

VEGF-C–VEGFR-3 signals induce Notch target genes through PI(3)K and FOXC2

To understand the mechanisms whereby VEGF-C–VEGFR-3 signalling contributes to Notch signalling, we stimulated cultured hBECs with VEGF-C and observed induction of Notch target genes over a 1–2 h stimulation period (Fig. 6a and data not shown). We found that VEGF-C induced *DLL4* in the hBECs (Supplementary Fig. S8), but similar induction of the Notch targets was observed also in the presence of a soluble Notch inhibitor, Dll4-Fc (Fig. 6a), implicating ligand-independent induction of Notch targets. Silencing VEGFR-3 expression with siRNA suppressed the induction of Notch targets and *DLL4* in response to VEGF-C (Fig. 6b). Interestingly, VEGF-C potentiated Notch target gene expression induced by transduction of hBECs with a retrovirus encoding membrane-bound Dll4 (Fig. 6c). The endothelial Notch receptors (*NOTCH1* and *NOTCH4*) were not induced by VEGF-C stimulation (Supplementary Fig. S8). Taken together, these data indicate that VEGF-C–VEGFR-3 signalling can induce Notch target genes through a mechanism that is independent of canonical Notch signalling.

Phosphatidylinositol 3-kinase (PI(3)K) is a downstream effector of receptor tyrosine kinases, and it has been implicated as a positive regulator of Notch signalling[36–38]. PI(3)K is activated by VEGFR-3 signals, indicating a mechanism for activation of Notch downstream of VEGFR-3. Indeed, pharmacological inhibition of PI(3)K, but not the MAP-kinase MEK, suppressed Notch activation by VEGF-C (Fig. 6d and data not shown). Interestingly, siRNA

silencing of VEGFR-3 expression returned ligand-induced activation of PI(3)K to baseline levels (Fig. 6e), indicating that PI(3)K activity is at least partially regulated by VEGFR-3 in angiogenic endothelial cells.

PI(3)K/Akt signalling is known to regulate FOX family transcription factors[39], and VEGFR-3 has been reported to genetically interact with FoxC2 in lymphatic endothelial cells[40]. FOXC2 has also been shown to directly regulate *HEY2* and *DLL4* expression[38,41], indicating a possible link between the VEGFR-3 and Notch signalling pathways. We found *FOXC2* messenger RNA induction in hBECs by VEGF-C stimulation, but not in response to Notch activation by membrane-bound Dll4 (Fig. 7a and data not shown). Loss of *Vegfr3 in vivo* led to a marked decrease in the level of FoxC2 expression in the endothelial cells at the angiogenic front (Fig. 7b–d). Downregulation of *Foxc2* was also evident in *Vegfc* heterozygous retinas (Fig. 7e). To investigate whether VEGFR-3 and FoxC2 function in the same pathway, we generated $Vegfr3^{+/-}$;$Foxc2^{+/-}$ compound heterozygous mice, which exhibited similar excessive endothelial growth, branching and filopodia projection as observed in the $Vegfr3^{i\Delta EC}$ homozygous retinas (Figs 7f–i, 1). The vasculature of single heterozygotes appeared indistinguishable from wild-type littermates (Fig. 7f–i). Collectively, these data indicate that VEGFR-3 may induce Notch target genes through FoxC2 independently of Notch ligand–receptor interactions (Fig. 7j).

DISCUSSION

Here we demonstrate that endothelial loss of VEGFR-3 leads to hypervascularization in developmental and tumour angiogenesis as well as in purely VEGF-driven angiogenesis. This finding contrasts with our previous data showing that VEGFR-3-blocking antibodies rather suppress angiogenesis[14,42]. Although seemingly in stark conflict, it is important to consider that the two phenotypes are a result of profoundly different perturbations of VEGFR-3. In the case of antibodies, the intracellular domain is free to interact with intracellular proteins, whereas the entire receptor is missing following genetic deletion.

Indeed, VEGFR-3 can be phosphorylated by the intracellular tyrosine kinase Src, activated downstream of integrins following cell adhesion to matrix collagen I, even in conditions in which VEGFR-3 tyrosine kinase activity is lost[33]. Here we showed that the tyrosine kinase domain of VEGFR-3 can be phosphorylated following endothelial cell adhesion to collagen I in the presence of specific antibodies that block ligand–receptor interactions. Given that endothelial cells adhere to collagen I during angiogenic invasion of tissues[43], it is likely that some phosphorylation of VEGFR-3 occurs also *in vivo* even in the presence of blocking antibodies or the absence of the ligand.

Our analysis of mice harbouring various allelic combinations of endothelial-cell-deleted (*i*Δ*EC*), kinase-dead mutant and wild-type *Vegfr3* allowed for a titration of both kinase activity and genetic dose of VEGFR-3. The combination of a 50% decrease in genetic dose and loss of kinase activity in the remaining allele (iΔEC/KD) represented a threshold for the degree of VEGFR-3 phosphorylation required for normal angiogenesis. Importantly, our previous results indicate that the kinase-dead mutant may exert dominant-negative activity[32], which is why it is likely not to precisely mimic the effect of VEGFR-3-blocking antibodies.

Our results indicate that VEGFR-3 controls Notch targets, but VEGFR-3 is also capable of inducing mitogenic signalling[14]. According to our model, the latter ‘active’ function is dependent on ligand binding and can be blocked by specific inhibitors, whereas the regulation of Notch can persist even in the presence of inhibitors (Fig. 7j). The elucidation of the ligand-independent, or ‘passive’, signalling modality may explain why compound

deletion of both VEGFR-3 ligands, *Vegfc* and *Vegfd*, does not recapitulate the early embryonic lethality of *Vegfr3* gene-targeted mice[17], and why VEGFR-3-blocking antibodies, which prevent ligand-dependent activation of the receptor, suppress angiogenesis[14].

Interestingly, we observed a slight increase in the level of VEGFR-2 activity in cultured cells in which VEGFR-3 expression was silenced, whereas robust overexpression of wild-type, kinase-dead or ligand-binding-defective VEGFR-3 decreased the level of VEGFR-2 phosphorylation following VEGF stimulation[44]. Furthermore, we showed that VEGFR-2-blocking antibodies were able to rescue the hypervascularity resulting from endothelial deletion of *Vegfr3*, although morphologically the vessels remained abnormal. These findings indicate that VEGFR-3, although not capable of binding to VEGF, may act as a negative regulator of VEGF–VEGFR-2 signalling. Interestingly, implications towards such an interaction were already made in an elegant study demonstrating that VEGF can bring VEGFR-2 and VEGFR-3 to close proximity without inducing VEGFR-3 phosphorylation[45]. Importantly, we did not detect differences in the level of VEGFR-2 phosphorylation following VEGF stimulation in the presence of VEGFR-3-blocking antibodies.

The previous observations[45] place VEGFR-3 in VEGF–VEGFR-2 signalling clusters on the endothelial cell membrane and in subsequent signalosomes, which are known to contain multiple membrane-bound molecules that modulate the activity of VEGFRs, including ephrin-B2 (refs 46,47), claudin-like protein 24 (ref. 48), neuropilin-1 (ref. 49) and VE-cadherin[50]. It is therefore possible that VEGFR-3-blocking antibodies sterically disrupt the cluster or promote receptor internalization in addition to suppressing ligand-activated VEGFR-3 kinase activity. Conversely, loss of VEGFR-3 would allow its molecular partners to interact with VEGFR-2, which may modulate the signalling properties of this potent endothelial kinase.

We detected a significant decrease in the expression of multiple Notch target genes and the Notch ligand Dll4 in the $Vegfr3^{i\Delta EC}$ retinas, and observed a rescue of the hypervascular phenotype following exogenous activation of the Notch signalling pathway. In contrast, VEGF-C was capable of inducing Notch target gene expression even in the presence of a potent Notch inhibitor, that is independently of the canonical Notch ligands, as well as potentiating the induction of Notch targets in response to Dll4–Notch interactions. Notch target gene induction stimulated by VEGF-C was suppressed by administration of a PI(3)K inhibitor, which has also been shown to suppress Notch target gene expression following stimulation with VEGF (refs 36,38) or cyclic adenosine monophosphate[37] (cAMP) in endothelial cells or endothelial cell progenitors, respectively.

We have previously established a genetic interaction for VEGFR-3 and FoxC2 in the regulation of lymphatic valve formation[40]. Previous studies have shown that FOXC2 directly regulates the expression of *DLL4* and *HEY2* (refs 38,41), possibly by interacting with the Notch intracellular domain[38] (NICD). Here we demonstrate that endothelial loss of *Vegfr3* leads to a pronounced downregulation of FoxC2, and $Foxc2^{+/-}$;$Vegfr3^{+/-}$ compound heterozygotes recapitulated the phenotype observed in $Vegfr3^{i\Delta EC}$ homozygotes. Interestingly, $Notch1^{+/-}$;$Vegfr3^{+/-}$ compound heterozygous embryos exhibit increased lethality, whereas single heterozygotes survive in normal Mendelian ratios[51]. According to our findings and the published literature, it seems that VEGFR-3 can augment Notch signalling independently of canonical Notch ligand–receptor interactions through a mechanism involving FoxC2.

In zebrafish, VEGF-C controls angiogenesis before the formation of the lymphatic vascular system[52]. Interestingly, we detected induction of VEGF-C expression in macrophages at

sites of sprout fusion, and robust expression in cells localized at vessel branch points. Tie2-positive macrophages have been implicated in tumour angiogenesis[53] and as chaperones of sprout fusion during development[24], which is why it is of particular interest that the Tie2-positive macrophages were also VEGF-C positive. We observed similar vascular mispatterning, branching failure and a decreased level of Notch target gene expression in both *Vegfc* haploinsufficient mice and macrophage-deficient *op/op* mice. Although macrophages produce a plethora of growth factors[26], our studies implicate VEGF-C as a key factor in vascular branch formation on the basis of genetic loss-of-function experiments, as well as the spatiotemporally coincident expression of both VEGF-C and VEGFR-3 at sites of sprout fusion.

Importantly, the phenotype resulting from heterozygous loss of *Vegfc* is different from homozygous endothelial deletion of *Vegfr3*, as characterized by decreased and increased branching, respectively. Deficiency of the ligand is likely to lead to decreased levels of activity of both VEGFR-3 and VEGFR-2, and to affect the 'active' mode of VEGFR-3 signalling, which promotes angiogenesis, whereas the passive mode of signalling is still able to function through intracellular activation of VEGFR-3. However, the loss of *Vegfr3* abolishes both signalling modalities, leading to a significant decrease in the level of Notch signalling. Unlike the loss of VEGF-C, which resulted in reduced angiogenesis, the loss of VEGFR-3 did not negatively affect VEGFR-2 signalling; rather a small increase was observed.

VEGFR-3 signals seem to have an important role in a mechanism for the rapid conversion of tip cells to stalk cells, which is required at points of sprout fusion, where tip cells of opposing sprouts meet and establish cell–cell junctions. Our data support a model in which VEGF-C-producing macrophages stimulate VEGFR-3-positive tip cells to turn on Notch target genes, which leads to decreased sensitivity to VEGF and downregulation of VEGFR-3 in these cells[14,27,28], facilitating the assembly of vascular loops. In support of this model, we observed FoxC2 expression only in stalk cells and in endothelial cells forming vascular loops, but not in tip cells. Interestingly, *Vegfc* expression is also found in angiogenic endothelial cells during development[14], indicating the possibility of autocrine VEGF-C–VEGFR-3 interactions that may produce qualitatively distinct signals.

Our data indicate that BECs are instructed to migrate and proliferate primarily by VEGFR-2, whereas VEGFR-3 is the primary receptor driving differentiation signals towards the stalk-cell phenotype by activating Notch target gene expression through FoxC2. However, when VEGFR-2 is blocked, VEGFR-3 kinase activity can partially compensate for the loss of VEGFR-2 activity in driving the growth of endothelial cells, and vice versa[14]. Indeed, we have previously shown that VEGFR-3 activation can promote proliferation of BECs *in vivo,* but these signals are weak when compared with those originating from VEGFR-2 (refs 14,54). However, blocking VEGFR-3 augmented the effect of VEGF–VEGFR-2 axis inhibitors by providing additional inhibition of angiogenesis[14], which reflects the capacity of VEGFR-3 for angiogenic signalling.

Our results using inducible gene targeting elucidate a bimodal function for VEGFR-3 in angiogenesis as a driver of both growth and differentiation of endothelial cells, which could not have been discovered by studying specific inhibitors alone, attesting to the power of mouse molecular genetics. VEGFR-3-blocking antibodies and kinase inhibitors are capable of targeting only the 'active' arm of VEGFR-3 signalling, whereas the 'passive' arm could be eliminated only by genetic deletion of the receptor (Fig. 7j). Our results support an intricate mechanism that controls the formation and integrity of vascular micro-anastomoses during angiogenesis, and reinforce the concept of augmentation of Notch signals by receptor

tyrosine kinase activation, which may provide additional tools for the therapeutic manipulation of the blood vascular system.

METHODS

Methods and any associated references are available in the online version of the paper at http://www.nature.com/naturecellbiology

Supplementary Material

Refer to Web version on PubMed Central for supplementary material.

Acknowledgments

We would like to thank T. Petrova (CePO, CHUV and University of Lausanne, Switzerland) for the *Foxc2*$^{+/-}$ mice, M. Achen and S. Stacker (Peter MacCallum Cancer Centre, Melbourne, Australia) for the *Vegfd*$^{-/-}$ mice, B. Pytowski at Eli Lilly for VEGFR-2-and VEGFR-3-blocking antibodies, M. Jeltsch (Molecular/Cancer Biology Laboratory, University of Helsinki, Finland) for generating VEGF-C antibodies, S. Kaijalainen (Molecular/Cancer Biology Laboratory, University of Helsinki, Finland) for generating mDll4-Fc and mDll4-ECTM-eGFP expression vectors, A. Alitalo (Institute of Pharmaceutical Sciences, ETH Zurich, Switzerland) for valuable help with experiments and K. Helenius for critical comments on the manuscript. The Biomedicum Molecular Imaging Unit is acknowledged for microscopy services, and N. Ihalainen, T. Laakkonen, K. Salo and T. Tainola for excellent technical assistance, as well as personnel of the Meilahti Experimental Animal Center (University of Helsinki) for expert animal husbandry. We also thank I. Rosewell (London Research Institute, UK) for generation of chimaeric mice. This work was supported by grants from the Academy of Finland, the Association for International Cancer Research, the Finnish Cancer Organizations, the Helsinki University Research Fund, the Sigrid Juselius Foundation, the Louis-Jeantet Foundation and the European Research Council (ERC-2010-AdG-268804-TX-FACTORS). T.T. was supported by personal grants from the Emil Aaltonen Foundation, the K. Albin Johansson Foundation, the Finnish Medical Foundation, the Maud Kuistila Foundation, the Orion-Farmos Research Foundation and the Paulo Foundation. G.Z. was supported by personal grants from the K. Albin Johansson Foundation, the Finnish Medical Foundation, The Paulo Foundation, the Ida Montin Foundation and the Orion-Farmos Research Foundation. H.G. was supported by Cancer Research UK, the Lister Institute of Preventive Medicine, the European Molecular Biology Organization (EMBO) Young Investigator Programme and the Leducq Transatlantic Network ARTEMIS. LJ. was supported by an EMBO long-term postdoctoral fellowship. C.A.F. was supported by a Marie Curie FP7 postdoctoral fellowship.

References

1. Ferrara N, et al. Heterozygous embryonic lethality induced by targeted inactivation of the VEGF gene. Nature. 1996; 380:438–442.
2. Carmeliet P, et al. Abnormal blood vessel development and lethality in embryos lacking a single VEGF allele. Nature. 1996; 380:435–439. [PubMed: 8602241]
3. Shalaby F, et al. Failure of blood island formation and vasculogenesis in Flk-1-deficient mice. Nature. 1995; 376:62–66. [PubMed: 7596435]
4. Gille H, et al. Analysis of biological effects and signaling properties of Flt-1 (VEGFR-1) and KDR (VEGFR-2). A reassessment using novel receptor-specific vascular endothelial growth factor mutants. J Biol Chem. 2001; 276:3222–3230. [PubMed: 11058584]
5. Tammela T, Alitalo K. Lymphangiogenesis: molecular mechanisms and future promise. Cell. 2010; 140:460–476. [PubMed: 20178740]
6. Dixelius J, et al. Ligand-induced vascular endothelial growth factor receptor-3 (VEGFR-3) heterodimerization with VEGFR-2 in primary lymphatic endothelial cells regulates tyrosine phosphorylation sites. J Biol Chem. 2003; 278:40973–40979. [PubMed: 12881528]
7. Nilsson I, et al. VEGF receptor 2/-3 heterodimers detected *in situ* by proximity ligation on angiogenic sprouts. EMBO J. 2010; 29:1377–1388. [PubMed: 20224550]
8. Dumont DJ, et al. Cardiovascular failure in mouse embryos deficient in VEGF receptor-3. Science. 1998; 282:946–949. [PubMed: 9794766]

9. Covassin LD, Villefranc JA, Kacergis MC, Weinstein BM, Lawson ND. Distinct genetic interactions between multiple Vegf receptors are required for development of different blood vessel types in zebrafish. Proc Natl Acad Sci USA. 2006; 103:6554–6559. [PubMed: 16617120]
10. Kaipainen A, et al. Expression of the *fms*-like tyrosine kinase FLT4 gene becomes restricted to lymphatic endothelium during development. Proc Natl Acad Sci USA. 1995; 92:3566–3570. [PubMed: 7724599]
11. Lohela M, Helotera H, Haiko P, Dumont DJ, Alitalo K. Transgenic induction of vascular endothelial growth factor-C is strongly angiogenic in mouse embryos but leads to persistent lymphatic hyperplasia in adult tissues. Am J Pathol. 2008; 173:1891–1901. [PubMed: 18988807]
12. Paavonen K, Puolakkainen P, Jussila L, Jahkola T, Alitalo K. Vascular endothelial growth factor receptor-3 in lymphangiogenesis in wound healing. Am J Pathol. 2000; 156:1499–1504. [PubMed: 10793061]
13. Valtola R, et al. VEGFR-3 and its ligand VEGF-C are associated with angiogenesis in breast cancer. Am J Pathol. 1999; 154:1381–1390. [PubMed: 10329591]
14. Tammela T, et al. Blocking VEGFR-3 suppresses angiogenic sprouting and vascular network formation. Nature. 2008; 454:656–660. [PubMed: 18594512]
15. Karkkainen MJ, et al. Vascular endothelial growth factor C is required for sprouting of the first lymphatic vessels from embryonic veins. Nat Immunol. 2004; 5:74–80. [PubMed: 14634646]
16. Baldwin ME, et al. Vascular endothelial growth factor D is dispensable for development of the lymphatic system. Mol Cell Biol. 2005; 25:2441–2449. [PubMed: 15743836]
17. Haiko P, et al. Deletion of vascular endothelial growth factor C (VEGF-C) and VEGF-D is not equivalent to VEGF receptor 3 deletion in mouse embryos. Mol Cell Biol. 2008; 28:4843–4850. [PubMed: 18519586]
18. Gerhardt H, et al. VEGF guides angiogenic sprouting utilizing endothelial tip cell filopodia. J Cell Biol. 2003; 161:1163–1177. [PubMed: 12810700]
19. Hellstrom M, et al. Dll4 signalling through Notch1 regulates formation of tip cells during angiogenesis. Nature. 2007; 445:776–780. [PubMed: 17259973]
20. Suchting S, et al. The Notch ligand Delta-like 4 negatively regulates endothelial tip cell formation and vessel branching. Proc Natl Acad Sci USA. 2007; 104:3225–3230. [PubMed: 17296941]
21. Roca C, Adams RH. Regulation of vascular morphogenesis by Notch signaling. Genes Dev. 2007; 21:2511–2524. [PubMed: 17938237]
22. Kamei M, et al. Endothelial tubes assemble from intracellular vacuoles *in vivo*. Nature. 2006; 442:453–456. [PubMed: 16799567]
23. Strilic B, et al. The molecular basis of vascular lumen formation in the developing mouse aorta. Dev Cell. 2009; 17:505–515. [PubMed: 19853564]
24. Fantin A, et al. Tissue macrophages act as cellular chaperones for vascular anastomosis downstream of VEGF-mediated endothelial tip cell induction. Blood. 2010; 116:829–840. [PubMed: 20404134]
25. Kubota Y, et al. M-CSF inhibition selectively targets pathological angiogenesis and lymphangiogenesis. J Exp Med. 2009; 206:1089–1102. [PubMed: 19398755]
26. Qian BZ, Pollard JW. Macrophage diversity enhances tumor progression and metastasis. Cell. 2010; 141:39–51. [PubMed: 20371344]
27. Siekmann AF, Lawson ND. Notch signalling limits angiogenic cell behaviour in developing zebrafish arteries. Nature. 2007; 445:781–784. [PubMed: 17259972]
28. Benedito R, et al. The notch ligands Dll4 and Jagged1 have opposing effects on angiogenesis. Cell. 2009; 137:1124–1135. [PubMed: 19524514]
29. Claxton S, et al. Efficient, inducible Cre-recombinase activation in vascular endothelium. Genesis. 2008; 46:74–80. [PubMed: 18257043]
30. Le Bras B, et al. VEGF-C is a trophic factor for neural progenitors in the vertebrate embryonic brain. Nat Neurosci. 2006; 9:340–348. [PubMed: 16462734]
31. Skobe M, et al. Concurrent induction of lymphangiogenesis, angiogenesis, and macrophage recruitment by vascular endothelial growth factor-C in melanoma. Am J Pathol. 2001; 159:893–903. [PubMed: 11549582]

32. Karkkainen MJ, et al. A model for gene therapy of human hereditary lymphedema. Proc Natl Acad Sci USA. 2001; 98:12677–12682. [PubMed: 11592985]
33. Galvagni F, et al. Endothelial cell adhesion to the extracellular matrix induces c-Src-dependent VEGFR-3 phosphorylation without the activation of the receptor intrinsic kinase activity. Circ Res. 2010; 106:1839–1848. [PubMed: 20431062]
34. Jakobsson L, et al. Endothelial cells dynamically compete for the tip cell position during angiogenic sprouting. Nat Cell Biol. 2010; 12:943–953. [PubMed: 20871601]
35. Wiktor-Jedrzejczak WW, Ahmed A, Szczylik C, Skelly RR. Hematological characterization of congenital osteopetrosis in op/op mouse. Possible mechanism for abnormal macrophage differentiation. J Exp Med. 1982; 156:1516–1527. [PubMed: 7130905]
36. Takeshita K, et al. Critical role of endothelial Notch1 signaling in postnatal angiogenesis. Circ Res. 2007; 100:70–78. [PubMed: 17158336]
37. Yamamizu K, et al. Convergence of Notch and β-catenin signaling induces arterial fate in vascular progenitors. J Cell Biol. 2010; 189:325–338. [PubMed: 20404113]
38. Hayashi H, Kume T. Foxc transcription factors directly regulate Dll4 and Hey2 expression by interacting with the VEGF-Notch signaling pathways in endothelial cells. PLoS One. 2008; 3:e2401. [PubMed: 18545664]
39. Burgering BM. A brief introduction to FOXOlogy. Oncogene. 2008; 27:2258–2262. [PubMed: 18391968]
40. Petrova TV, et al. Defective valves and abnormal mural cell recruitment underlie lymphatic vascular failure in lymphedema distichiasis. Nat Med. 2004; 10:974–981. [PubMed: 15322537]
41. Norrmen C, et al. FOXC2 controls formation and maturation of lymphatic collecting vessels through cooperation with NFATc1. J Cell Biol. 2009; 185:439–457. [PubMed: 19398761]
42. Laakkonen P, et al. Vascular endothelial growth factor receptor 3 is involved in tumor angiogenesis and growth. Cancer Res. 2007; 67:593–599. [PubMed: 17234768]
43. Davis GE, Senger DR. Endothelial extracellular matrix: biosynthesis, remodeling, and functions during vascular morphogenesis and neovessel stabilization. Circ Res. 2005; 97:1093–1107. [PubMed: 16306453]
44. Zhang L, et al. VEGFR-3 ligand-binding and kinase activity are required for lymphangiogenesis but not for angiogenesis. Cell Res. 2010; 20:1319–1331. [PubMed: 20697430]
45. Nilsson I, et al. VEGF receptor 2/-3 heterodimers detected *in situ* by proximity ligation on angiogenic sprouts. EMBO J. 2010; 29:1377–1388. [PubMed: 20224550]
46. Wang Y, et al. Ephrin-B2 controls VEGF-induced angiogenesis and lymphangiogenesis. Nature. 2010; 465:483–486. [PubMed: 20445537]
47. Sawamiphak S, et al. Ephrin-B2 regulates VEGFR2 function in developmental and tumour angiogenesis. Nature. 2010; 465:487–491. [PubMed: 20445540]
48. Saharinen P, et al. Claudin-like protein 24 interacts with the VEGFR-2 and VEGFR-3 pathways and regulates lymphatic vessel development. Genes Dev. 2010; 24:875–880. [PubMed: 20439428]
49. Whitaker GB, Limberg BJ, Rosenbaum JS. Vascular endothelial growth factor receptor-2 and neuropilin-1 form a receptor complex that is responsible for the differential signaling potency of VEGF(165) and VEGF(121). J Biol Chem. 2001; 276:25520–25531. [PubMed: 11333271]
50. Carmeliet P, et al. Targeted deficiency or cytosolic truncation of the VE-cadherin gene in mice impairs VEGF-mediated endothelial survival and angiogenesis. Cell. 1999; 98:147–157. [PubMed: 10428027]
51. Shawber CJ, et al. Notch alters VEGF responsiveness in human and murine endothelial cells by direct regulation of VEGFR-3 expression. J Clin Invest. 2007; 117:3369–3382. [PubMed: 17948123]
52. Ober EA, et al. Vegfc is required for vascular development and endoderm morphogenesis in zebrafish. EMBO Rep. 2004; 5:78–84. [PubMed: 14710191]
53. De Palma M, Venneri MA, Roca C, Naldini L. Targeting exogenous genes to tumor angiogenesis by transplantation of genetically modified hematopoietic stem cells. Nat Med. 2003; 9:789–795. [PubMed: 12740570]

54. Mäkinen T, et al. Isolated lymphatic endothelial cells transduce growth, survival and migratory signals via the VEGF-C receptor VEGFR-3. EMBO J. 2001; 20:4762–4773. [PubMed: 11532940]
55. Soriano P. Generalized lacZ expression with the ROSA26 Cre reporter strain. Nat Genet. 1999; 21:70–71. [PubMed: 9916792]
56. Iida K, et al. Essential roles of the winged helix transcription factor MFH-1 in aortic arch patterning and skeletogenesis. Development. 1997; 124:4627–4638. [PubMed: 9409679]
57. Pytowski B, et al. Complete and specific inhibition of adult lymphatic regeneration by a novel VEGFR-3 neutralizing antibody. J Natl Cancer Inst. 2005; 97:14–21. [PubMed: 15632376]
58. Prewett M, et al. Antivascular endothelial growth factor receptor (fetal liver kinase 1) monoclonal antibody inhibits tumor angiogenesis and growth of several mouse and human tumors. Cancer Res. 1999; 59:5209–5218. [PubMed: 10537299]
59. Weijzen S, et al. The Notch ligand Jagged-1 is able to induce maturation of monocyte-derived human dendritic cells. J Immunol. 2002; 169:4273–4278. [PubMed: 12370358]
60. Tammela T, et al. Angiopoietin-1 promotes lymphatic sprouting and hyperplasia. Blood. 2005; 105:4642–4648. [PubMed: 15746084]
61. Baluk P, et al. Pathogenesis of persistent lymphatic vessel hyperplasia in chronic airway inflammation. J Clin Invest. 2005; 115:247–257. [PubMed: 15668734]
62. Ruhrberg C, et al. Spatially restricted patterning cues provided by heparin-binding VEGF-A control blood vessel branching morphogenesis. Genes Dev. 2002; 16:2684–2698. [PubMed: 12381667]
63. Karpanen T, et al. Lymphangiogenic growth factor responsiveness is modulated by postnatal lymphatic vessel maturation. Am J Pathol. 2006; 169:708–718. [PubMed: 16877368]
64. Zheng W, et al. Notch restricts lymphatic vessel sprouting induced by vascular endothelial growth factor. Blood. 2011; 118:1154–1162. [PubMed: 21566091]
65. Tvorogov D, et al. Effective suppression of vascular network formation by combination of antibodies blocking VEGFR ligand binding and receptor dimerization. Cancer Cell. 2010; 18:630–640. [PubMed: 21130043]
66. Jussila L, et al. Lymphatic endothelium and Kaposi's sarcoma spindle cells detected by antibodies against the vascular endothelial growth factor receptor-3. Cancer Res. 1998; 58:1599–1604. [PubMed: 9563467]
67. Ghalamkarpour A, et al. Recessive primary congenital lymphoedema caused by a VEGFR3 mutation. J Med Genet. 2009; 46:399–404. [PubMed: 19289394]
68. Persaud K, et al. Involvement of the VEGF receptor 3 in tubular morphogenesis demonstrated with a human anti-human VEGFR-3 monoclonal antibody that antagonizes receptor activation by VEGF-C. J Cell Sci. 2004; 117:2745–2756. [PubMed: 15150322]
69. Karpanen T, et al. Functional interaction of VEGF-C and VEGF-D with neuropilin receptors. FASEB J. 2006; 20:1462–1472. [PubMed: 16816121]
70. Jakobsson L, et al. Heparan sulfate in trans potentiates VEGFR-mediated angiogenesis. Dev Cell. 2006; 10:625–634. [PubMed: 16678777]
71. Lobov IB, et al. Delta-like ligand 4 (Dll4) is induced by VEGF as a negative regulator of angiogenic sprouting. Proc Natl Acad Sci USA. 2007; 104:3219–3224. [PubMed: 17296940]

METHODS

Mice and tissues

The study was approved by the Committee for Animal Experiments of the District of Southern Finland. The mice were anaesthetized with intraperitoneal injections of xylazine (10 mg kg^{-1}) and ketamine (80 mg kg^{-1}). The *Vegfr3*$^{+/LacZ}$ (ref. 8), *Vegfr3*$^{flox/flox}$ (ref. 17), *Vegfc*$^{+/LacZ}$ (ref. 15), *Vegfd*$^{+/-}$ (ref. 16), ROSA26-R (ref. 55), *Foxc2*$^{+/-}$ (ref. 56), *Csf1*$^{op/op}$ (ref. 35) and *Pdgfb–iCreER*^{T2} (ref. 29) mouse lines have been published previously. After killing the mice, tissues were immersed in 4% paraformaldehyde, washed in phosphate buffered saline (PBS) and then processed for whole-mount staining, immersed in OCT

medium (Tissue Tek) or embedded in paraffin. Deletion of *Vegfr3* in the *Pdgfb–iCreER^{T2}*;*Vegfr3$^{flox/flox}$* mice was validated by immunohistochemistry and qRT-PCR (Supplementary Fig. S1). The possibility of a 3′ *Vegfr3* mRNA fragment originating from a cryptic start codon was excluded by qRT-PCR probes targeting the 5′ and 3′ ends of the *Vegfr3* transcript; no difference in expression levels was found (data not shown).

Analysis of angiogenesis in the postnatal mouse retina and in the embryonic mouse hindbrain

Neonatal *Pdgfb–iCreER^{T2}*; *Vegfr3$^{flox/flox}$*, *Pdgfb–iCreER^{T2}*;*ROSA26-R* or control mice were intragastrically injected with 2 μl of 4-OHT (Sigma) dissolved in 97% ethanol, on P3 and P4 using a 10 μl Hamilton syringe. A 12 h induction of Cre activity with 4-OHT during P5 was sufficient to result in Cre-activated β-galactosidase reporter expression in most endothelial cells of the developing retinal vasculature; the strongest signal was observed in the tip cells (Supplementary Fig. S1a), which express high levels of *Pdgfb* (ref. 18). Induction for 48 h resulted in robust Cre-dependent β-galactosidase activity in all endothelial cells (Supplementary Fig. S1b). For the antibody treatments, NMRI pups were subcutaneously injected with 50 mg kg^{-1} of anti-VEGFR-3 (mF4-31C1; ref. 57) or anti-VEGFR-2 (DC101; ref. 58) on P3 and P4. The small peptide mimetic of the Notch ligand Jagged1 (Jag1) or scrambled control peptide (SC-Jag1, Thermo Scientific) was dissolved in 50% dimethylsulphoxide and 50% sterile water, and administered subcutaneously at 10 mg kg^{-1} (refs 19,59) on P3 and P4 at 12 h intervals. To identify proliferating endothelial cells, the pups were given 0.2 mg of 5-bromo-2-deoxyuridine (BrdU) by intraperitoneal injections, 2 h before being killed. In all cases, the pups were killed on P5, and their eyes were collected for analysis. For hindbrain analysis, pregnant females were given 2.5 mg of 4-OHT dissolved in 40% ethanol and 60% sunflower seed oil (Sigma), using a feeding needle at E10.5 (for 24 h analysis) or E10.5 and E11.5 (for 48 h analysis). Embryos were collected on E11.5 or E12.5, and hindbrains were processed for whole-mount immunohistochemistry.

Transduction of the mouse ear skin with adenoviral gene transfer vectors

Cre was induced at least 2 days in advance by subcutaneous implantation of sustained release pellets (21 days) containing tamoxifen (25 mg, Innovative Research). Adenoviruses encoding human $VEGF_{165}$ or $VEGF\text{-}B_{167}$ were injected intradermally into the ears of *Pdgfb–iCreER^{T2}*;*Vegfr3$^{flox/flox}$* mice. A total of 2×10^8 plaque-forming units of each virus were injected in a volume of 50 μl. The mice were perfusion-fixed 5 days after injection, and the ears were collected and processed for whole-mount analysis[60], or immersed in OCT medium (Tissue Tek).

Tumour cell lines, xenografts and treatments

B16–F10–Luc2–G5 mouse melanoma or mouse LLC cells were maintained in DMEM, supplemented with 2 mM L-glutamine, penicillin (100 U ml^{-1}), streptomycin (100 μg ml^{-1}) and 10% fetal calf serum (Promo Cell). For B16–F10–Luc2–G5 cells, zeocin was added at a final concentration of 0.3 mg ml^{-1} as a selection marker. The B16 and LLC syngeneic grafts were made by injecting $2–4\times10^6$ cells into the subcutaneous space in the abdominal flank of *Pdgfb–iCreER^{T2}*;*Vegfr3$^{flox/flox}$* mice. Again, Cre was induced by subcutaneous implantation of the sustained tamoxifen-release pellets (25 mg, Innovative Research).

Immunohistochemistry

50 μm sections of tumours and 10 μm sections of ears were fixed with cold acetone, washed with PBS and blocked with TNB (PerkinElmer). The following primary antibodies were

used for immunostaining of mouse tissues: polyclonal goat anti-mouse VEGFR-3 (R&D Systems, 1:50–1:100), rabbit polyclonal anti-GFP (TP401, Torrey Pines Biolabs, 1:1,000), unconjugated or fluorescein isothiocyanate (FITC)-conjugated rat anti-PECAM-1 (clone MEC 13.3, 553370, BD Pharmingen, 1:500, 1:800), rat anti-mouse endomucin (V.7C7: sc-65495, Santa Cruz Biotechnology, 1:100), polyclonal rabbit anti-FITC (Zymed/Invitrogen, 1:100), rabbit anti-mouse collagen IV (LB-1403, Cosmo Bio, 1:1,000), rabbit #6 polyclonal antiserum to VEGF-C (ref. 61), or pre-immune rabbit #6 serum as a negative control[61], and Alexa-Fluor-594-conjugated mouse anti-BrdU monoclonal antibody (clone MoBU-1, B35132, Invitrogen, 1:500). Sections were washed with TNT buffer and the primary antibodies were detected with the appropriate Alexa 488, 594 or 647 secondary antibody conjugates (Molecular Probes/Invitrogen).

Hindbrains of E11.5 or E12.5 embryos were processed for whole-mount immunofluoresence staining as previously described[62]. For analysis of the microvasculature, retinas were stained with biotinylated *Griffonia simplicifolia* lectin (Vector Laboratories), as before[18], followed by immunostaining. Alternatively, to detect β-galactosidase activity, eyes were processed, as before[14]. After staining, retinas were washed and mounted in Vectashield (Vector Laboratories) or re-fixed in 4% paraformaldehyde and processed for whole-mount immunofluoresence staining. All fluorescently labelled samples were mounted with Vectashield containing 4,6-diamidino-2-phenylindole (DAPI, Vector Laboratories).

Microscopy

Fluorescently labelled samples were analysed with a compound fluorescent microscope (Zeiss 2, Carl Zeiss; ×10 objective with numerical aperture (NA) 0.30) or a confocal microscope (Zeiss LSM 510Meta, objectives ×10 with NA 0.45, oil objectives ×40 with NA 1.3 and ×63 with NA 1.4; or Zeiss LSM 5 Duo, objectives ×10 with NA 0.45, oil objectives ×40 with NA 1.3 and ×63 with NA 1.4) using multichannel scanning in frame mode, as before[14]. Three-dimensional projections were digitally reconstructed from confocal *z* stacks. Co-localization of signals was assessed from single confocal optical sections. Images of whole retinas were acquired using tile scanning with a pinhole diameter >3.0 Airy units. X-gal (5-bromo-4-chloro-3-indolyl-β-D-galactoside) staining of LacZ reporter mice was analysed with a Leica DM LB camera (objectives ×10 with NA 0.25 and ×20 with NA 0.4).

Cell culture and reagents

hBECs (PromoCell) were maintained in endothelial cell growth medium (ECGM, PromoCell, C22120) with supplements provided by the manufacturer. For stimulation experiments, hBECs were starved for 6–8 h in serum-free ECGM and stimulated for 1 or 2 h in fresh starvation media. The following reagents were used: human VEGF (100 ng ml^{-1}, 293-VE, R&D) and VEGF-$C^{\Delta N\Delta C}$ (200 ng ml^{-1}; ref. 63). For Notch or PI(3)K inhibition experiments, cells were starved for 6 h and Dll4-Fc (Dll4-Fc conditioned medium[64]), LY294002 (10 μM, 440204, Calbiochem) or PD98059 (20 μM, Calbiochem) was added for 30, 15 and 30 min respectively before stimulation with VEGF-C (200 ng ml^{-1}, added in the same media). For silencing experiments, hBECs were transfected with human *VEGFR3* or non-targeted siRNA (Thermo Scientific Dharmacon siGENOME ON-TARGETplus SMARTpool reagents), using Oligofectamine (Invitrogen). For activation of Notch in cultured hBECs, 50% of the cells were transduced with pMX retroviral vectors expressing mouse Dll4–ECTM–eGFP (mDll4–ECTM–eGFP; ref. 64). Gene expression was examined 48 h post-transfection by qRT-PCR from cells lysed in RLT buffer (Qiagen). Alternatively, cells were lysed in PLCLB lysis buffer (150 mM NaCl, 5% glycerol, 1% Triton X-100, 1.5 M $MgCl_2$, 50 mM HEPES, pH 7.5, 1 mM Na_3VO_4, phenylmethylsulphonyl fluoride, leupeptin and aprotinin) for western blotting[65], using the following antibodies: goat anti-

mouse VEGFR-2 (AF357, R&D Systems), goat anti-mouse VEGFR-3 (AF743, R&D Systems), mouse anti-human VEGFR-3 (clone 9D9, ref. 66), rabbit anti-human β-actin (#4967, Cell Signaling) and mouse anti-phosphotyrosine (#05-321, Millipore).

Analysis of VEGFR-3 phosphorylation following adhesion to collagen I

hBECs were transfected with pMX retrovirus encoding VEGFR3–StreptagII (ref. 67), detached using Accutase (PAA Laboratories) and plated on Collagen I or poly-L-lysine (both 4 μg cm^{-2}), which was used as a control. Cells were then incubated for the indicated times depending on the experimental set-up with 1 μg ml^{-1} 3C5 (ref. 68), 1 nM cediranib (Astra Zeneca) or 1 mM PP2 (Calbiochem). VEGFR-3 was precipitated from PLCLB lysates using Strep-Tactin beads (IBA). After that proteins were analysed by western blotting using antibodies to pTyr or VEGFR-3.

Analysis of VEGFR-3 and VEGFR-2 phosphorylation in *ex vivo* embryo cultures

E10.5–E11.5 NMRI wild-type embryos were excised from amnionic sacs and placed in Dulbecco's modified Eagle's medium (DMEM) containing 0.2% bovine serum albumin (BSA) on ice. The embryos were injected through the outflow tract with 0.5 ml of DMEM containing 100 ng ml^{-1} recombinant human $VEGF_{165}$ (R&D Systems), 200 ng ml^{-1} VEGF-$C^{\Delta N\Delta C}$ (ref. 69) or 0.2% BSA. Altogether 10–15 embryos were used in each group. Embryos were placed in DMEM containing the same concentration of growth factors, incubated at 37 °C for 20 min and lysed in 1% Triton X-100, 40 mM Tris-HCl (pH 7.5), 150 mM NaCl, 2 mM Na_3VO_4, 100 μM phenylmethylsulphonyl fluoride, 50 mM NaF and 10 μg ml^{-1} of both aprotinin and leupeptin. Insoluble materials were removed by centrifugation at 14,000*g* for 15 min.

PI(3)K activity assay

hBECs were incubated on 96-well plates (10^4 cells per well) and silenced with human *VEGFR3* or non-targeting siRNA for 48 h, before stimulating with VEGF (100 ng ml^{-1}) or VEGF-C (200 ng ml^{-1}) for 15 min. PI(3)K activity was evaluated using FACE PI3-kinase p85 ELISA Kit (Active Motif) according to the manufacturer's instructions. The signal was normalized to cell numbers by staining with crystal violet. PI(3)K activity was measured with a microplate reader (Thermo Labsystems Multiscan Ascent).

Three-dimensional cultures of embryoid bodies

Embryonic stem cells were routinely cultured on a layer of irradiated DR4 mouse embryonic fibroblasts in the presence of leukaemia inhibitory factor (LIF). For vascular sprouting experiments, cells were cultured for two passages without feeders, trypsinized, depleted of LIF, followed by mixing of wild-type (DsRed) and $Vegfr3^{+/LacZ}$ cells in a 1:1 ratio and left in suspension (day 0). On day 4, embryoid bodies were embedded in a polymerized collagen I gel (as previously described[70]) with the addition of 30 ng ml^{-1} $mVEGF_{164}$ (Peprotech) with dimethylsulphoxide or DAPT (5 μM, Sigma-Aldrich). Medium was changed on day 6 and every day thereafter.

qRT-PCR

Total RNA from retinas, collected at P5, or hBECs was isolated using the RNeasy Mini Kit (Qiagen) or the NucleoSpin RNA II Kit (Macherey-Nagel). Homogenization was carried out using rotor-stator homogenization, followed by on-column DNase digestion (RNase-Free

DNase Set, 79254). Quality control of samples was carried out using a Nanodrop ND-1000 spectrophotometer. RNA was reverse-transcribed using the DyNAmo cDNA Synthesis Kit (F-470L, Finnzymes) or the iScript cDNA Synthesis Kit (Bio-Rad) according to the manufacturer's instructions. Three qRT-PCR reactions were carried out from every *in vitro* transcription reaction using TaqMan Gene Expression Assays (Applied Biosystems) and the DyNAmo Probe qPCR Kit (F-450S, Finnzymes) or the iQ Supermix Kit (Bio-Rad). qRT-PCR was carried out using a BIO-RAD C1000 Thermal cycler according to a standardized protocol. The TaqMan Gene Expression Assays used for mouse mRNA were: *Gapdh* (4352932E), *Cadh5* (Mm00486938_m1), *Pdgfb* (Mm00440678_m1), *Vegfr1* (Mm00438980_m1), *5′-Vegfr3* (Mm01292608_m1), *3′-Vegfr3* (Mm00433354_m1), *Nrarp* (Mm00482529_s1), *Hey1* (Mm00468865_m1), *Hey2* (Mm00469280_m1), *Dll4* (Mm00444619_m1), *Notch1* (Mm00435245_m1), *Notch4* (Mm00440525_m1) and *Foxc2* (Mm01250130_s1). At least three retinas from *Pdgfb–iCreER*^{T2}; *Vegfr3*$^{flox/flox}$ and *Vegfr3*$^{flox/flox}$ littermates were used for analysis at P5.

The TaqMan Gene Expression Assays used for human RNA were: *GAPDH* (Hs99999905_m1), *HEY1* (Hs01114113_m1), *HEY2* (Hs00232622_m1), *NRARP* (Hs01104102_s1), *DLL4* (Hs01117332_g1), *NOTCH1* (Hs01062014_m1), *NOTCH4* (Hs00965895_g1) and *FOXC2* (Hs00270951_s1). The data were normalized to the endogenous controls *Gapdh* or *Cadh5* and *GAPDH* in murine and human samples, respectively. At least three independent experiments per condition were analysed. Fold changes were calculated using the comparative CT (threshold cycle) method.

Vessel morphometry and quantitative analysis

The vascular surface area in retinas was quantified as an isolectin-B4-positive area from ×10 confocal micrographs acquired of all intact quarters of the processed retina and at a similar distance from the optic nerve using Image J software, as described previously[14]. PECAM-1-positive vessels from thick tumour sections were quantified from 1.69 mm^2 micrographs from regions of uniform staining intensity in a similar manner. PECAM-1-positive vessels in the ear sections were quantified from images that were acquired using tile-scanning mode with a pinhole diameter >3 Airy units. Vessel branching points, sprouts and filopodia number were counted manually from fluorescence micrographs of retinas, as described previously[71]. For each hindbrain, the number of sprouting vessels on the pial side and the number of branching points on the subventricular zone were determined in 3–6 randomly chosen 0.85 mm^2 fields. At least two litters of embryos per embryonic stage were independently analysed. Images were edited using PhotoShop software (Adobe).

Statistical analysis

Statistical analysis was carried out using PASW Statistics 18.0. A two-tailed Student *t*-test, paired Student *t*-test or one-way analysis of variance (ANOVA) was used for statistical analysis. A *P* value of less than 0.05 was considered to be statistically significant.

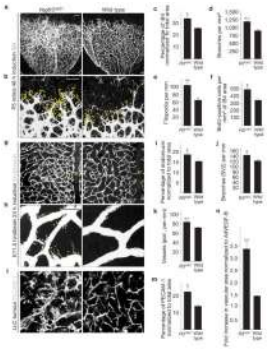

Figure 1.

Blood vascular hyperplasia and excessive filopodia projection in mice with a targeted deletion of *Vegfr3* in the endothelium. (**a,b**) Visualization of blood vessels by isolectin B4 (iB4) staining of $Vegfr3^{i\Delta EC}$ and wild-type littermate retinas at P5. Yellow dots indicate filopodia at the vascular front in **b**. Scale bars, 100 μm (**a**) and 50 μm (**b**). (**c–f**) Quantitative analysis of the retinas shown in **a** and **b**. (**c**) iB4-positive surface area normalized to total area. (**d**) Number of vessel branching points. (**e**) Number of filopodia per length of vascular front. (**f**) BrdU-positive cells per iB4 area (see Supplementary Fig. S2). In all cases, Cre activity was induced for 48 h before the mice were killed. **c–e** show data from one litter containing 5 $Vegfr3^{i\Delta EC}$ and 3 wild-type mice. (**f**) Data from one litter containing 3 $Vegfr3^{i\Delta EC}$ and 4 wild-type mice. (**g,h**) Endomucin staining of E11.5 mouse hindbrains after Cre induction for 24 h before the mice were killed. Yellow asterisks indicate the hindbrain midline in **g**, and yellow dots indicate filopodia in **h**. Scale bars, 100 μm (**g**) and 20 μm (**h**). (**i–k**) Quantitative analysis of the $Vegfr3^{i\Delta EC}$ and wild-type hindbrains; n =3 $Vegfr3^{i\Delta EC}$ and 5 wild-type embryos. (**i**) Endomucin-positive surface area normalized to total area. (**j**) Number of vessel branching points in the subventricular side. (**k**) Number of vessel sprouts in the pial side (see Supplementary Fig. S3). (**l**) PECAM-1 staining of LLC tumour xenografts 11 days after implantation into $Vegfr3^{i\Delta EC}$ or wild-type littermate mice. Scale bar, 50 μm. (**m**) Quantification of PECAM-1-positive area in the tumours shown in **l**; n = 5 $Vegfr3^{i\Delta EC}$ and 5 wild-type mice. (**n**) Fold increase in vascular area 4 days after transduction with adenoviral vectors encoding VEGF (AdVEGF), normalized to AdVEGF-B in $Vegfr3^{i\Delta EC}$ versus wild-type mice (see Supplementary Fig. S4); n =3 ears per group. $^{**}P$ <0.005, $^{*}P$ <0.05. Error bars, s.e.m.

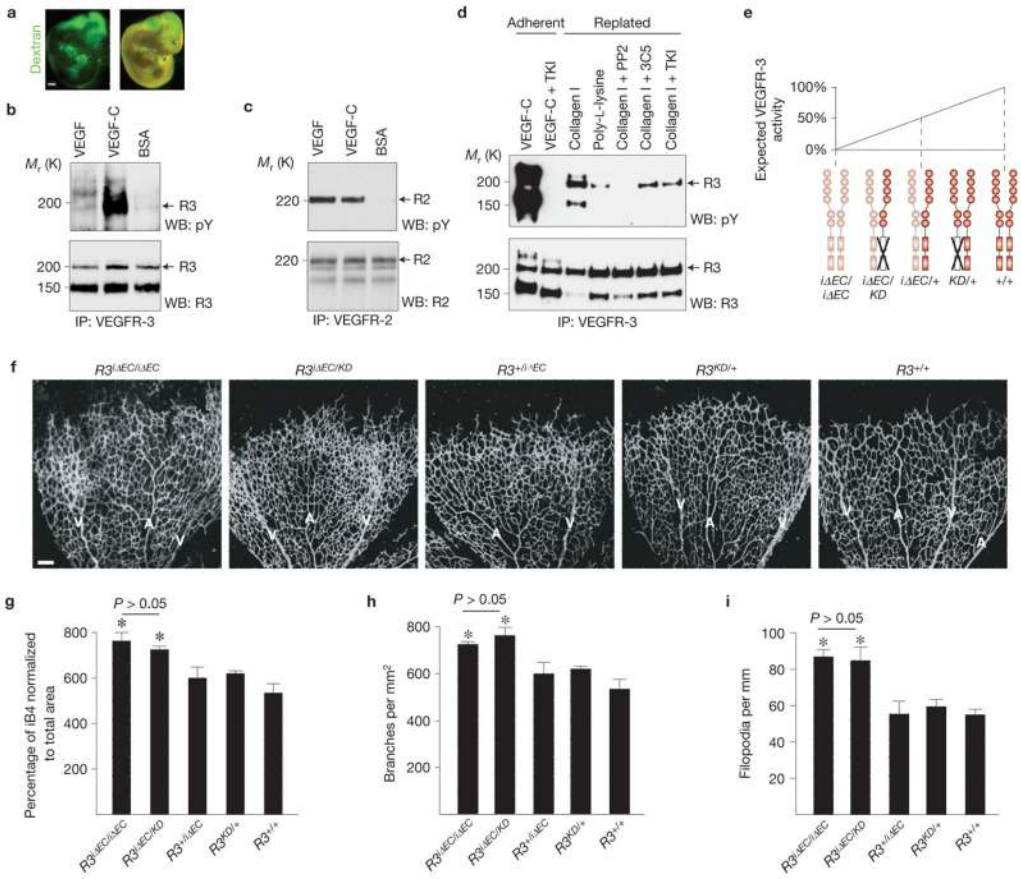

Figure 2.

Role of VEGFR-3 tyrosine kinase activity in angiogenesis. (**a**) Intra-embryonic injection of FITC–dextran (green) into the cardiac outflow tract at E11.5 showing homogeneous perfusion of the embryo. Scale bar, 200 μm. (**b,c**) Immunoprecipitation (IP) of VEGFR-3 (**b**) or VEGFR-2 (**c**) of embryos stimulated with VEGF, VEGF-C or BSA followed by western blotting (WB) for phosphotyrosine (pY), VEGFR-3 (R3) or VEGFR-2 (R2). $N = 9$ (**b**) and 8 (**c**) embryos per lane. (**d**) Immunoprecipitation of VEGFR-2 from hBECs transduced with pMX–VEGFR3–StreptagII retrovirus. Adherent cells were stimulated with VEGF-C, whereas detached cells were replated on collagen I or poly-L-lysine, and subjected to the indicated inhibitors. Uncropped images of blots are shown in Supplementary Fig. S9a. (**e**) Schematic illustration showing the expected VEGFR-3 activity following the indicated genetic perturbations of *Vegfr3*. (**f**) iB4 staining of mouse retinas at P5 48 h after 4-OHT administration. A, artery; V, vein. Scale bar, 100 μm. (**g–i**) Quantitative analysis of the retinas shown in **f**. (**g**) Isolectin B4 (iB4)-positive surface area normalized to total area. (**h**) Number of vessel branching points. (**i**) Number of filopodia per length of vascular front. Data pooled from 4 litters containing altogether 8 *iΔEC/iΔEC,* 4 *iΔEC/KD,* 6 *+/iΔEC*, 5 *KD/+* and 7 wild-type pups. $^{*}P<0.05$. Error bars, s.e.m.

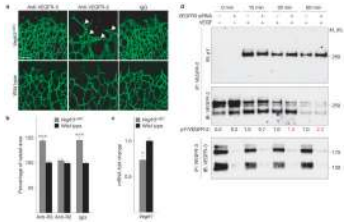

Figure 3.

An increased level of VEGFR-2 signalling contributes to vascular hyperplasia in *Vegfr3*$^{i\Delta EC}$ retinas. (**a**) Isolectin B4 staining (in green) of *Vegfr3*$^{i\Delta EC}$ retinas after treatment with VEGFR-3- or VEGFR-2-blocking antibodies during P3–P5. Non-specific rat IgG was used as a control. Arrowheads indicate abnormally thick vessels. Scale bar, 100 μm. (**b**) Statistical analysis showing the percentage vessel area increase in *Vegfr3*$^{i\Delta EC}$ versus wild-type littermate mice in every treatment group (individual experiments; $n = 4$, 5 and 4 *Vegfr3*$^{i\Delta EC}$ pups treated with anti-VEGFR-3, anti-VEGFR-2 and IgG, respectively; and 6, 3 and 5 wild-type pups treated with anti-VEGFR-3, anti-VEGFR-2 and IgG, respectively). (**c**) qRT-PCR analysis of *Vegfr1* gene (also known as *Flt1*) expression; $n = 4$ *Vegfr3*$^{i\Delta EC}$ and 3 wild-type pups. In all analyses of the retina, Cre activity was induced for 48h before the mice were killed. $^{*}P < 0.05$, $^{***}P < 0.001$. Error bars, s.e.m. (**d**) Cultured HUVECs subjected to siRNA-mediated silencing of *VEGFR3* expression (*VEGFR3* siRNA) and stimulation with VEGF for the indicated times. VEGFR-2 was immunoprecipitated (IP) followed by immunoblotting (IB) for phosphotyrosine (pY) and VEGFR-2. Numbers below the blots indicate relative intensities of pY to VEGFR-2, normalized to control siRNA at the same time point. Note the increased pVEGFR-2 signal at 30 min and 60min (red). Immunoprecipitation and western blot analysis for VEGFR-3 from the same lysates is shown below. Uncropped images of blots are shown in Supplementary Fig. S9b.

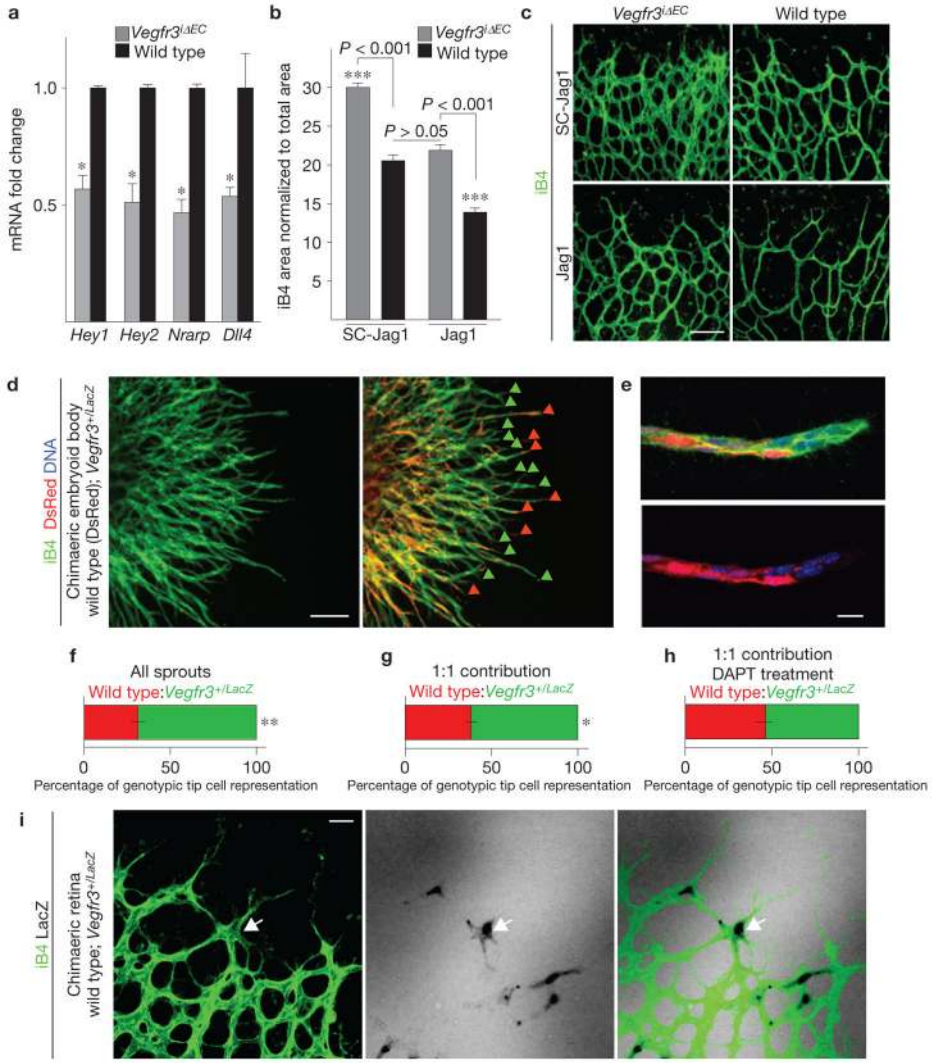

Figure 4.

A decreased level of Notch signalling underlies excessive angiogenesis in *Vegfr3*$^{i\Delta EC}$ retinas. (**a**) Fold changes in *Hey1, Hey2, Nrarp* and *Dll4* mRNA levels in the retinas of *Vegfr3*$^{i\Delta EC}$ and wild-type littermate pups at P5. mRNA levels were normalized to *Cadh5* to compensate for the increased endothelial cell numbers in *Vegfr3*$^{i\Delta EC}$ retinas. $^{*}P < 0.05$; n = 4 *Vegfr3*$^{i\Delta EC}$ and 3 wild-type pups. Error bars, s.e.m. (**b,c**) Vessel area quantification (**b**) and isolectin B4 (iB4) staining (**c**) of *Vegfr3*$^{i\Delta EC}$ and wild-type littermate retinas at P5 following administration of Jagged1 peptide mimetics (Jag1) or scrambled peptides (SC-Jag1) and 4-OHT for 48h. Scale bar, 100 μm. $^{***}P < 0.001$; n = 3 *Vegfr3*$^{i\Delta EC}$ and 4 wild-type pups treated with SC-Jag1 and 4 *Vegfr3*$^{i\Delta EC}$ and 4 wild-type pups treated with Jag1. Data pooled from 2 individual experiments. Error bars, s.e.m. (**d**) A 10 day chimaeric embryoid body derived from wild-type DsRed-expressing embryonic stem cells (red), mixed in a 1:1 ratio with embryonic stem cells having one functional *Vegfr3* allele (*Vegfr3*$^{+/LacZ}$) and stained for iB4 (green). Red arrowheads indicate tip cells of wild-type origin; green arrowheads point to *Vegfr3* heterozygous cells. Scale bar, 200 μm. (**e**) High-magnification image of a sprout showing a mosaic distribution of the cells. DNA in blue. Scale bar, 20 μm. (**f,g**) Quantification of the tip cell genotype in all sprouts (**f**; 65.89%±2.5% s.e.m.; n = 621 sprouts), in sprouts that exhibited a 1:1 contribution of wild-type and *Vegfr3*$^{+/LacZ}$ cells (**g**;

61.8%± 1.8% s.e.m.; n = 360 sprouts) and in sprouts with a 1:1 contribution of wild-type and *Vegfr3*$^{+/LacZ}$ cells following treatment with DAPT (**h**; 53.7%±2.7% s.e.m.; n = 325 sprouts). $^{**}P < 0.01$, $^{**}P < 0.05$. Error bars, s.e.m. (**i**) Mosaic retina of a P5.5 pup derived from a wild-type blastocyst injected with *Vegfr3*$^{+/LacZ}$ embryonic stem cells and stained for iB4. β-galactosidase activity (in black, arrow) indicates a *Vegfr3*$^{+/LacZ}$ cell. Scale bar, 50 μm.

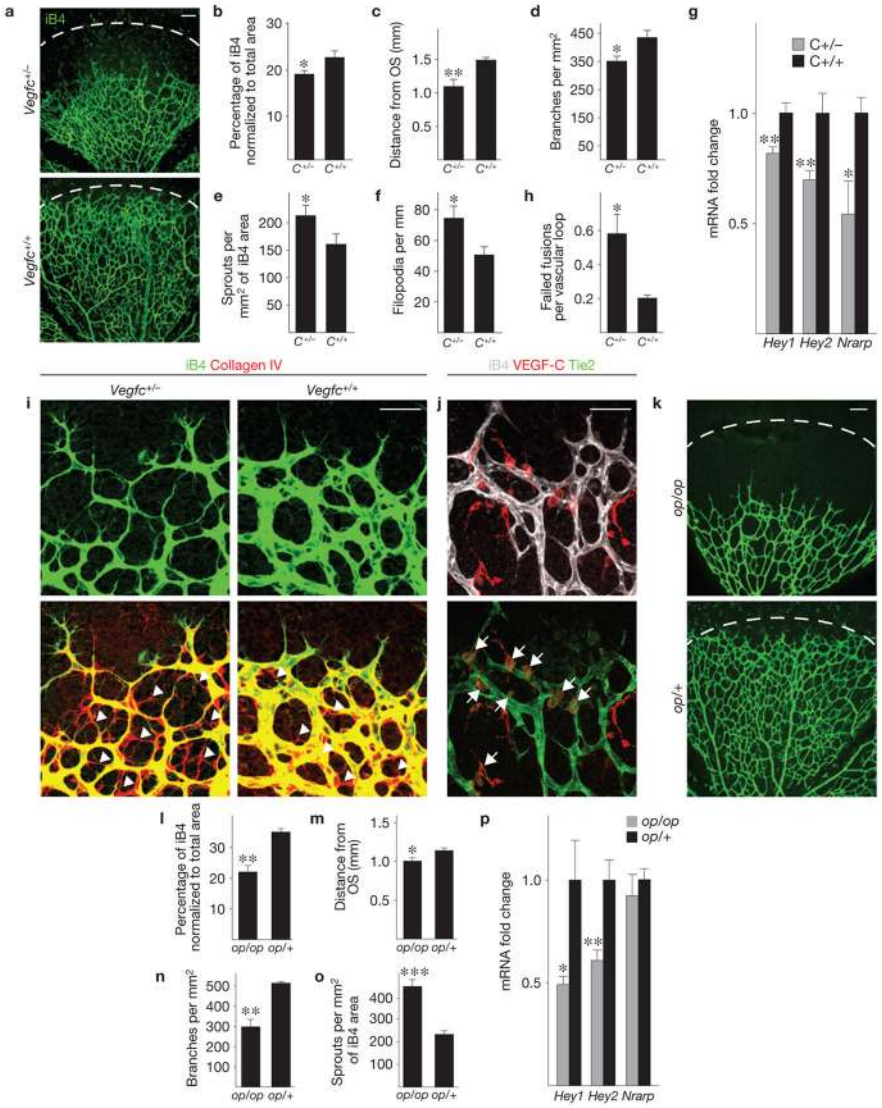

Figure 5.

Vegfc haploinsufficiency leads to instability of sprout fusion points and inefficient angiogenesis. (**a**) Isolectin B4 (iB4) staining (green) of retinas from *Vegfc*$^{+/-}$ mice and their wild-type littermates at P5. (**b–f**) Quantitative analysis of the retinas shown in **a**; data pooled from two litters containing altogether 6 *Vegfc*$^{+/-}$ and 9 wild-type pups. (**b**) iB4-positive surface area normalized to total area. (**c**) Extent of vascular plexus migration from the optic stalk (OS). (**d**) Number of vessel branching points. (**e**) Number of sprouts. (**f**) Filopodia per length of vascular front. (**g**) Fold changes in *Hey1*, *Hey2* and *Nrarp* mRNA levels analysed by qRT-PCR in the retinas of *Vegfc*$^{+/-}$ and wild-type pups at P5 (data pooled from two litters containing altogether 7 *Vegfc*$^{+/-}$ and 6 wild-type pups). (**h**) Number of failed fusions per vascular loop in the retinas of *Vegfc*$^{+/-}$ and *Vegfc*$^{+/+}$ pups at P5 (n = 6 *Vegfc*$^{+/-}$ and 9 wild-type pups, data pooled from 2 litters). (**i**) iB4 (green) and collagen IV (red) staining of *Vegfc*$^{+/-}$ or wild-type littermate retinas at P5. Arrowheads indicate empty basement membrane sleeves. (**j**) iB4 (white), VEGF-C (red) and Tie2 (green) immunostaining in wild-type mouse retinas at P5. Arrows indicate VEGF-C- and Tie2-positive macrophages at the angiogenic front. (**k**) iB4 staining (green) of P5 retinas of *op/op* pups and *op/+* littermate controls. (**l–o**) Quantitative analysis of the retinas shown in **k**; n = 5 *op/op* and 4 *op/+* pups.

Dashed line in **a** and **k** indicates a similar distance from the optic stalk (OS). (**l**) iB4-positive surface area normalized to total area. (**m**) Extent of vascular plexus migration from the optic stalk. (**n**) Number of vessel branching points. (**o**) Number of sprouts. (**p**) Fold changes in *Hey1, Hey2* and *Nrarp* mRNA levels analysed by qRT-PCR in the retinas of *op/op* pups and *op/+* pups at P5 *(n* = 5 *op/op* and 3 *op/+* pups). Scale bars, 100 μm (**a,k**) and 50 μm (**i,j**). * $P < 0.05$, ** $P < 0.01$, $^{***}P < 0.001$. Error bars, s.e.m.

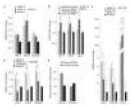

Figure 6.

VEGF-C promotes Notch signalling in endothelial cells through VEGFR-3 and PI(3)K. (**a–d**) Fold changes in Notch target gene and *DLL4* levels in hBECs stimulated with 200 ng ml^{-1} VEGF-C, and treated with Dll4-Fc conditioned medium (**a**), transfected with *VEGFR3* siRNA or control siRNA (**b**), in conditions where 50% of hBECs express membrane-bound Dll4 (Dll4-TM; **c**) or treated with the PI(3)K inhibitor LY294002 (**d**). Cells were stimulated for 1 h before lysis. Expression of *GAPDH* was used as the normalization control. Note the successful transduction of hBECs with retroviruses encoding Dll4-TM in **c**, as evaluated by qRT-PCR. (**e**) Fold increase in PI(3)K activity in *VEGFR3* versus control silenced hBECs after stimulation with VEGF-C (100 ng ml^{-1}) for 15 min. Data pooled from 2 individual experiments, each containing 3 replicates. * denotes *P* values versus control group ($^{*}P$ <0.05, $^{**}P$ <0.01, $^{***}P$ <0.001) and # denotes *P* values between groups (# *P* <0.05, ## *P* <0.01). Error bars, s.e.m.

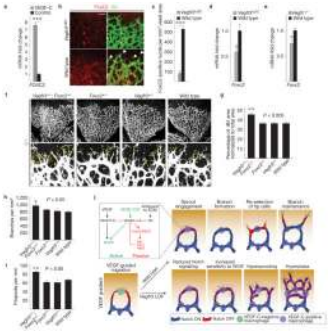

Figure 7.

VEGFR-3 interacts with the transcription factor FoxC2 to control angiogenesis. (**a**) Fold change in the level of *FOXC2* mRNA expression following stimulation of hBECs with 200 ng ml^{-1} VEGF-C (n = 3 plates per group). (**b**) Immunostaining for FoxC2 (red) and isolectin B4 (iB4; green) in $Vegfr3^{i\Delta EC}$ and wild-type littermate pups at P5. Arrowheads indicate FoxC2-negative tip cells. (**c**) Quantification of FoxC2-positive nuclei from the retinas shown in **b**. Nuclei in the area of iB4-positive endothelial cells were quantified at the angiogenic front (n = 3 pups per group). (**d,e**) Fold change in the level of *Foxc2* mRNA expression in $Vegfr3^{i\Delta EC}$ and wild-type littermate retinas (**d**), and in $Vegfc^{+/-}$ or wild-type littermate retinas (**e**) at P5 (n = 3 pups per group). (**f**) iB4 staining (white) in $Foxc2^{+/-}$; $Vegfr3^{+/-}$, $Foxc2^{+/-}$, $Vegfr3^{+/-}$ or wild-type littermate retinas at P5. Yellow dots in the lower panels indicate filopodia. (**g–i**) Quantitative analysis of the retinas shown in **f**. (**g**) iB4-positive surface area normalized to total area. (**h**) Number of vessel branching points. (**i**) Filopodia per length of vascular front. Data pooled from 2 litters; n = 3 $Foxc2^{+/-}$; $Vegfr3^{+/-}$, 4 $Foxc2^{+/-}$, 4 $Vegfr3^{+/-}$ and 4 wild-type pups. Scale bars, 50 μm. $^{*}P<0.05$, $^{**}P<0.01$, $^{***}P<0.001$. Error bars, s.e.m. (**j**) Schematic of VEGF-C-expressing macrophages in vessel anastomosis and branch maintenance during developmental angiogenesis. Initially, 2 tip cells that lead vascular sprouts are chaperoned to fuse by a macrophage (green). VEGF-C expression (purple) ensues in the macrophage, activating VEGFR-3 in the tip cells, which leads to the expression of Notch target genes and decreased sensitivity to the VEGF gradient in the cells. *Vegfr3* loss-of-function (LOF) leads to decreased Notch signalling. A simplified summary of the ‘active’ (green) and ‘passive’ (red) signalling pathways originating from VEGFR-3 is shown in the upper left corner. Only the ‘active’ pathway is targetable by inhibitors.